Engineering Structures 168 (2018) 950–966

Contents lists available at ScienceDirect

Engineering Structures

journal homepage: www.elsevier.com/locate/engstruct

Improved model for human induced vibrations of high-frequency floors

A.S. Mohammed[a,*], A. Pavic[a], V. Racic[b]

[a] Vibration Engineering Section, College of Engineering, Mathematics and Physical Sciences, University of Exeter, North Park Road, EX4 4QF Exeter, UK
[b] Department of Civil and Environmental Engineering, Politecnico di Milano, Piazza Leonardo da Vinci 32, 20133 Milan, Italy

ARTICLE INFO

Keywords:
Vibration serviceability
Walking excitation
Cut-off frequency
Probabilistic modelling

ABSTRACT

The key UK design guidelines published by the Concrete Society and Concrete Centre for single human walking excitation of high-frequency floors were introduced more than 10 years ago. The corresponding walking force model is derived using a set of single footfalls recorded on a force plate and it features a deterministic approach which contradicts the stochastic nature of human-induced loading, including intra- and inter- subject variability. This paper presents an improved version of this force model for high-frequency floors with statistically defined parameters derived using a comprehensive database of walking force time histories, comprising multiple successive footfalls that are continuously measured on an instrumented treadmill. The improved model enables probability-based prediction of vibration levels for any probability of non-exceedance, while the existing model allows for vibration prediction related to 75% probability of non-exceedance for design purposes. Moreover, the improved model shifts the suggested cut-off frequency between low- and high-frequency floors from 10 Hz to 14 Hz. This is to account for higher force harmonics that can still induce the resonant vibration response and to avoid possible significant amplification of the vibration response due to the near-resonance effect. Minor effects of near-resonance are taken into account by a damping factor. The performance of the existing and the improved models is compared against numerical simulations carried out using a finite element model of a structure and the treadmill forces. The results show that while the existing model tends to overestimate or underestimate the vibration levels depending on the pacing rate, the new model provides statistically reliable estimations of the vibration responses. Hence, it can be adopted in a new generation of the design guidelines featuring a probabilistic approach to vibration serviceability assessment of high-frequency floors.

1. Introduction

The advancements in construction materials and design software have boosted the current architectural trend of building lighter structures than ever with increasingly longer spans and reduced carbon footprint. While the Ultimate Limit State (ULS) requirements for these modern structures are normally met, Serviceability Limit State (SLS) criteria increasingly govern design. This is particularly the case with vibration serviceability of structures due to human activities, such as walking, running and jumping [1,2].

Building floors have traditionally been designed mainly to accommodate people, who are by their nature very sensitive vibration receivers [3]. Nowadays there is a growing need for floors accommodating vibration sensitive equipment, such as microscopes and lasers in hospitals and hi-tech laboratories. Their optimal functioning commonly permits extremely low vibration levels (often micro-levels) of the supporting structure which are far below human perception. Vibration criteria (VC) for sensitive equipment is normally provided by the manufacturer, leaving the provision of the adequate floor to clients and structural designers [2].

Early studies made vibration assessment based on static deflection of a floor and suggested increasing the stiffness and therefore the fundamental frequency to reduce the vibration response. The same concept features the work by Ungar and White [4] who were the first to use an "idealised footfall force" [5] in a method to calculate the maximum velocity response. This method has been further developed by Amick [6] and adopted in a number of design guidelines [7,8].

A more sophisticated approach was based on the nature of the vibration response [9,10]. If the response is dominated by a resonant build-up they are known as *low-frequency floors*, while those that show a sequence of transient responses due to each successive footfall are called *high-frequency floors*. The division between low- and high-frequency floors depends on whether the fundamental frequency of the floor is relatively low or high, respectively. The threshold frequency (known as *cut-off frequency)* varies significantly for different authors and design guidelines, as shown in Table 1.

* Corresponding author.
E-mail address: asm221@exeter.ac.uk (A.S. Mohammed).

https://doi.org/10.1016/j.engstruct.2018.04.093

Available online 18 May 2018

Table 1
Cut-off frequency between low- and high-frequency floors adopted by different authors and design guidelines.

Author	Cut-off frequency
Ohlsson [36]	8 Hz
Wyatt and Dier [9]	7 Hz
Allen and Murray [37]	9 Hz
The concrete society [27]	10 Hz
The concrete centre [38]	10 Hz
The Steel Construction Institute P354 [39]	10 Hz for general floors, open plan offices, etc. 8 Hz for enclosed spaces, e.g. operating theatre, residential
American institute of steel construction [26]	9 Hz

Floors supporting sensitive equipment are required to have low-level transient vibration responses due to human walking excitation [11,12], thus they should be high-frequency floors. A number of studies [13,14] reported that the cut-off frequencies given in Table 1 are too conservative, which has a major effect on the design and cost of ultra-sensitive facilities. They showed that the resonant build-up response can occur even for floors with a fundamental frequency of above 15 Hz [14]. This is because there are higher dominant harmonics of walking loading at frequencies above 10 Hz, which contain a significant amount of energy. For example, according to the design guidelines, a floor with a fundamental frequency of 11.5 Hz is a high-frequency floor. However, a person walking at a pacing rate 2.3 Hz, whose corresponding walking force has Fourier amplitudes shown in Fig. 1, still can induce the resonant vibrations by the harmonic corresponding to the fifth integer multiple of walking loading. This error in the floor type yields an underestimated vibration response, hence a floor may not be fit for purpose.

The uncertainty linked to the cut-off frequency could be explained by the lack of knowledge and/or reliable experimental data pertinent to human walking excitation. This study addresses this issue by determining a cut-off frequency based on detailed numerical analysis featuring a large number of continuously measured walking forces generated by many people walking on an instrumented treadmill [15,16]. Another major drawback of the available design guidelines is the deterministic mathematical description of human-induced loading, while a probabilistic approach is arguably more suitable due to the inherent stochastic nature of human walking forces [16–19]. This study proposes an improved and probability-based version of the widely used Arup's force model for high-frequency floors [20]. This model was chosen as it provides closest and least conservative predictions of floor vibrations compared with experimental results [12,14,21,22]. The parameter estimation of the proposed model and the model implementation take statistical approaches. Moreover, the effect of structural damping is introduced in this model to take into account any "near-resonance" effects.

For high-frequency floors, the time domain modelling approach used here is more appropriate than the frequency domain approach used elsewhere [17,23,24] due to its capability to describe the peak responses corresponding to footfall strikes. The performance of the new model has been verified via numerical simulations utilising the treadmill forces and a finite element model of a high-frequency floor.

Section 2 of this paper describes the nature of the human-induced vibration responses and the procedure followed to derive a more reliable cut-off frequency between low- and high-frequency floors. The new model and its implementation procedure are elaborated in Section 3, while its verification is demonstrated in Section 4. Finally, a discussion of the results and the main conclusions are presented in Section 5.

2. Resonant and transient vibration responses due to human walking excitation

This section demonstrates the nature of the resonant and transient vibration responses due to human walking excitation based on numerical simulations using measured walking forces (Section 2.1) applied to different Single Degree of Freedom (SDOF) oscillators (Section 2.2). Moreover, it aims to derive a reliable value of the cut-off frequency (Section 2.3) relevant to the model development presented in Section 4.

2.1. Walking forces

The authors have at their disposal a comprehensive database of 715 continuously measured vertical force time histories, generated by more than 70 test subjects walking individually on an instrumented treadmill [15,16]. Each test subject followed the same test protocol designed to record a force signal at a constant speed of rotation of the treadmill belts per each test. The speed was varied randomly from slow to fast across successive tests, so the database comprises forces for a wide range of pacing rates. Each force time history contains at least 60 successive footfalls, rather than a single footfall only used in development of Arup's model. This makes it possible to study the intra-subject variability of the walking loads, i.e. the inability of a person to generate two identical footfalls during a walking test. The large number of test

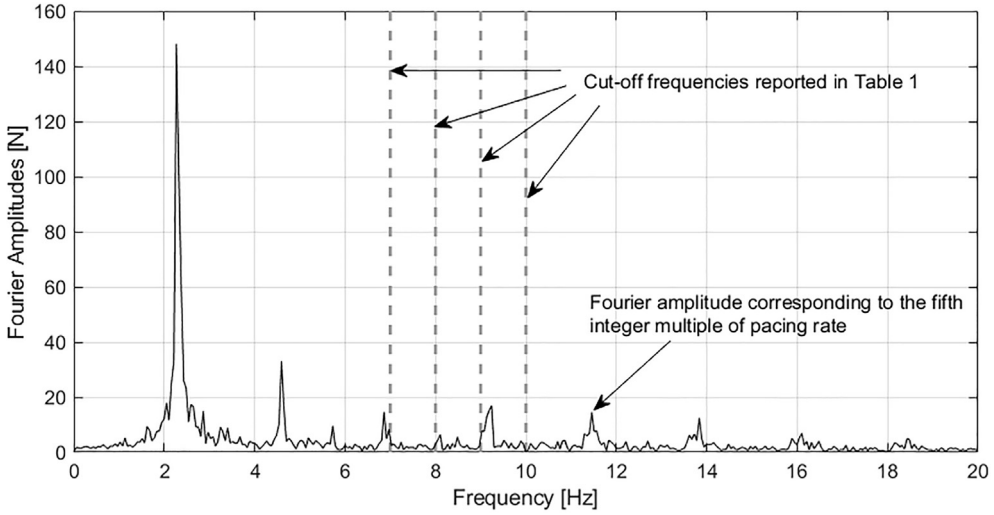

Fig. 1. Fourier amplitudes of a walking force signal measured using an instrumented treadmill corresponding to a pacing rate of 2.3 Hz.

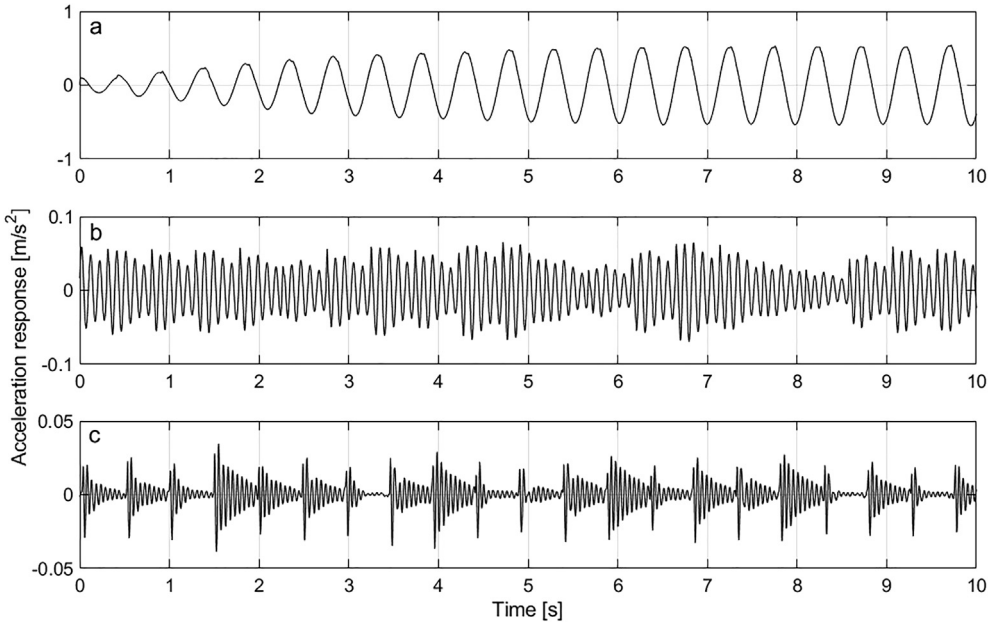

Fig. 2. Simulated vibration responses due to a recorded walking force with f_p = 2.0 Hz and natural frequency of the oscillator (a) f_n = 2.0 Hz, (b).

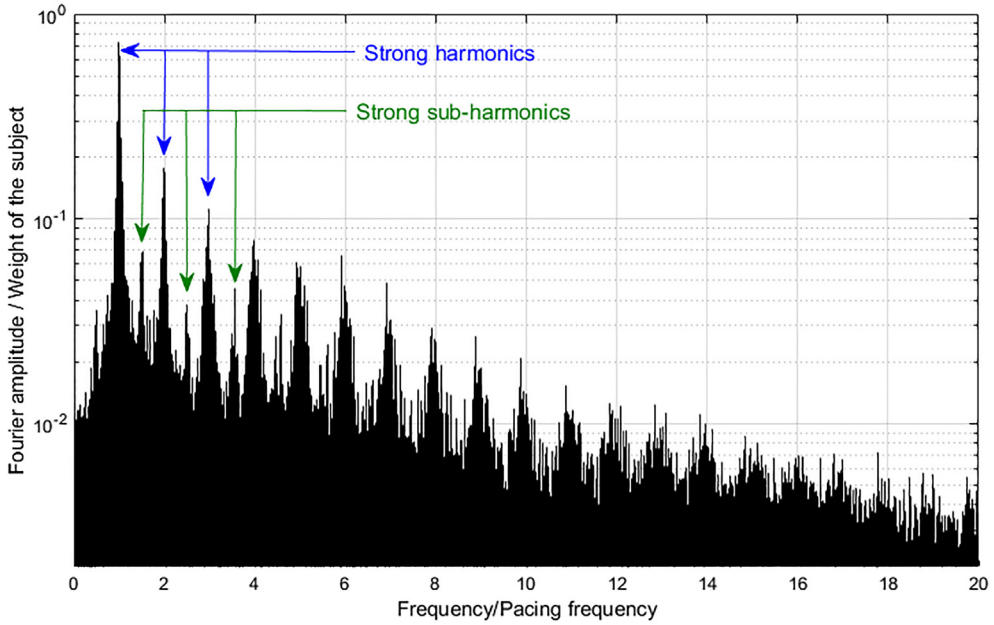

Fig. 3. Normalised discrete Fourier amplitudes for all available walking forces [15,16] with pacing rates between 1.4 and 2.5 Hz.

subjects processed in the experiment enables studies of inter-subject variability, i.e. differences between force records generated by different people under (nominally) identical conditions. These forces can be considered statistically more reliable data than that used in the development of the original Arup model [25].

The range of pacing rates corresponding to these walking forces is between 1.4 and 2.5 Hz. The force signals were cropped for the time duration of 50 footfalls from the middle of the force signal. Several first and last footfalls were discarded to eliminate potential negative effects related to the start and the end of the walking test, yielding footfalls that might not reliably represent the real walking of a person. This length of the force signal was used everywhere else in this paper unless otherwise stated. Moreover, the effect of body weight was excluded by normalising the forces [15,16] to 750 N before they were used in the analysis presented.

2.2. Resonant and transient vibration responses

Depending on the natural frequency (f_n) of the first vibration mode, the vibration response due to human walking excitation can take three distinct shapes (Fig. 2):

- When the fundamental frequency is relatively small (i.e. f_n < 8–10 Hz) and close to one of the integer multiples of the pacing rate (f_p), a resonant build-up response is likely to occur (Fig. 2a).
- If the fundamental frequency is much higher than the pacing rate (i.e. $f_n \gg f_p$) a transient response will dominate the vibration response (Fig. 2c).
- When the fundamental frequency lies between the two above mentioned ranges, the sharp transient decays are reduced

considerably, and the overall vibration levels are increased (Fig. 2b).

This paper focuses on modelling the transient vibration response (Fig. 2c), which is the typical case for high-frequency floors.

Besides the natural frequency, the behaviour of the vibration response is affected by the harmonics of the walking force that excite the dominant vibration modes of the structure [26,27]. The common knowledge is that a build-up of the resonant response is unlikely to occur if the fundamental frequency is higher than three or four integer multiples of the pacing rate [26,27]. The normalised Fourier amplitudes of all the forces in the database [15,16], for a length of 20.48 s, are overlapped in Fig. 3 with a logarithmic scale in its vertical axis. There is no apparent sign that beyond, say, 10 Hz (see Table 1) the Fourier amplitudes of the harmonics do not exist and cannot produce a resonant build-up response. They are smaller in amplitude, but they definitely exist at integer multiples of the pacing rate.

To assess the effect of the harmonics of the walking excitation on the vibration response, each walking force from the database was applied to a series of SDOF oscillators, which had natural frequencies between 1 and 40 Hz with an increment of 0.1 Hz. Therefore, the total number of the oscillators is 391 and the total number of simulated vibration responses is 279,565. The modal mass was assumed 1 kg and the damping ratio was assumed 3% in all simulations. The duration of each simulation is equal to the length of the corresponding walking force time history, while the integration time step is 0.005 s. For the response of each simulation, the running 1-s root mean square (1-s RMS) was calculated as described in Eq. (1).

$$v_{RMS} = \sqrt{\frac{1}{T}\int_0^T v^2(t)dt}, \tag{1}$$

where v_{RMS} is the velocity 1-s RMS (m/s) and T is the duration of the averaging (1-s).

The maximum transient vibration value (MTVV), which is equal to the maximum 1-s RMS, corresponding to each simulation was used for comparison, as shown in Fig. 4. The grey colour represents the MTVV velocity corresponding to each walking force and varying SDOF natural frequencies, while the black colour represents the average MTVV velocity at each SDOF natural frequency.

The MTVV velocity is relatively high at integer multiples of pacing rates (Fig. 4). This is the case even for the oscillators, with a natural frequency of up to 30 Hz. Therefore, there is no evidence that the harmonics of walking forces, which correspond to frequencies above the reported cut-off frequency in the design guidelines (Table 1), cannot induce a resonant build-up response. This implies that a more detailed study should be carried out to derive the cut-off frequency, as elaborated in the next section.

2.3. Determining cut-off frequency between low- and high-frequency floors

As already observed above, a typical transient response due to walking comprises a series of velocity peaks corresponding to heel strikes, followed by a decaying vibration response to around zero before the beginning of the next footfall, as shown in Fig. 2c [14]. This means that the response due to previous footfalls has a negligible contribution to the response due to the present footfall. On the other hand, for non-transient vibration responses (Fig. 2a and b), the response is affected by a number of previous footfalls depending on the structural damping.

Theoretically speaking, a transient response time history can be reconstructed from the peak responses followed by an exponentially decaying response in between them. In this case, the reconstructed vibration response level is similar to that of the original time history response (Fig. 5). Therefore, the proposed methodology to identify the cut-off frequency is as follows:

- Simulate vibration responses by applying measured walking forces [15,16] on SDOF oscillators with different natural frequencies.
- For each response time history, extract the peak velocity responses corresponding to each footfall strike with their exact times.
- Use the peak velocities to reconstruct the time history response which comprises only a decaying response after each peak velocity, as shown in Fig. 5.
- Establish the difference between the original and the reconstructed responses by calculating the ratio of their MTVVs (i.e. MTVV velocity of the reconstructed response over that for the original response).
- Repeat this process for the different natural frequencies of the SDOF oscillator and the measured walking forces [15,16].
- Identify the frequency corresponding to a value of the MTVV ratio which is reasonably close to 1.0, as explained below.

The closer the MTVV ratio to 1.0, the more similar are the reconstructed response and its corresponding simulated transient response. Fig. 6 compares two cases when the MTVV ratio is close or far from 1.0. The process of generating reconstructed vibration responses was repeated for all available walking forces [15,16] when the natural frequency of the SDOF oscillator is an integer multiple of the pacing rate (up to 20 Hz). This is to consider the effect of the harmonics at these frequencies. The damping ratio used in the simulations was 3% while the modal mass was assumed 1 kg. The MTVV ratios corresponding to this analysis are presented as box plots in Fig. 7. The upper and lower ends of the rectangles represent the values corresponding to a 75% and 25% chance of non-exceedance, respectively. The whiskers (ends of the extended lines from the boxes) represent the maximum and minimum values.

At relatively low pacing rates, the MTVV ratio approaches 1.0 at a lower SDOF natural frequency than that for higher pacing rates (Fig. 7). This indicates the dependency of the cut-off frequency on the pacing rates. For natural frequencies at or above 14 Hz, the median of the MTVV ratios for all pacing rates (horizontal lines in the middle of the rectangles in Fig. 7) were within 10% of 1.0 (i.e. 0.90–1.10), which is reasonably close to 1.0. This implies that the shape of vibration responses corresponding to SDOF oscillators with natural frequencies above 14 Hz resemble typical transient responses regardless of the pacing rate. The harmonics of walking forces [15,16] corresponding to frequencies above 14 Hz are more likely to increase the amplitude of the vibration responses rather than to induce a clear resonant build-up response. Therefore, this frequency has been selected as the cut-off frequency above which the human-induced vibration of floors is dominated by transient response.

3. Modelling human-induced vibrations of high-frequency structures

This section starts with necessary details of Arup's deterministic force model (Section 3.1), followed by its expansion into a more sophisticated probability-based successor proposed in this study (Sections 3.2 and 3.3) and its implementation in vibration serviceability assessment of high-frequency floors (Section 3.4).

3.1. Arup's model

The model was derived using a database of over 800 single footfalls recorded for 40 individuals stepping on a force plate while walking at a range of pacing rates controlled by a metronome [25]. The measured footfalls were shifted repeatedly along the time axes to synthesise the corresponding artificial and perfectly periodic force time history (Fig. 8). Each such force was applied to a series of SDOF oscillators with natural frequencies of 10–40 Hz and only the peak velocity for each simulation was extracted. The modal mass was assumed 1 kg for all simulations, so that the peak velocity response was numerically equivalent to the impulse represented by the shaded area in Fig. 8 and expressed in Ns. Such an impulse is termed *effective impulse*.

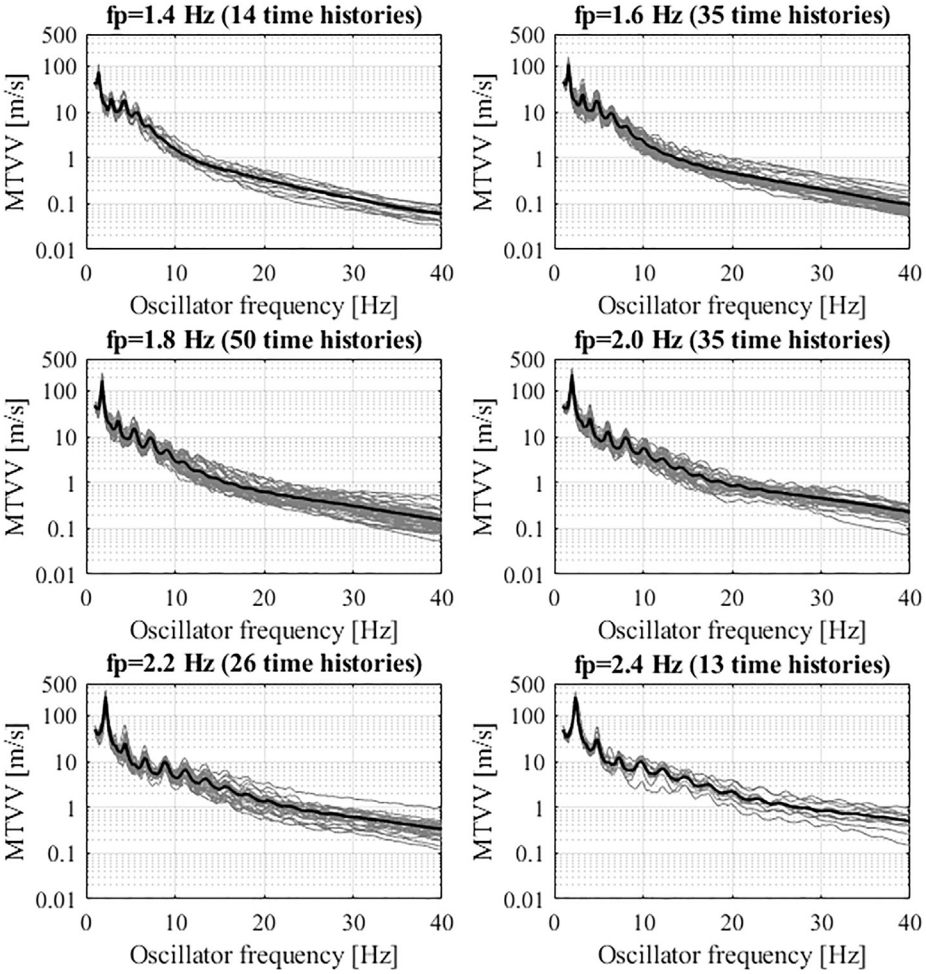

Fig. 4. MTVV velocity (grey) for pacing rates (f_p) from 1.4 Hz (up left) to 2.4 Hz (bottom right). Black represents the average MTVV velocity at each natural frequency.

For varying pacing rates, the mean of the extracted effective impulses are shown in Fig. 9 as a function of the 'floor frequency (Hz)', which is the natural frequency of the 1 kg SDOF system. The corresponding curve fit is:

$$I_{eff} = A\frac{f_p^{1.43}}{f_n^{1.3}}, \tag{2}$$

where, I_{eff} is the effective impulse (Ns), f_p is the pacing rate (Hz), f_n is the SDOF natural frequency (Hz) and A is a coefficient which has a mean value of 42 and a standard deviation of 0.4 while its corresponding design value for 75% chance of non-exceedance is 54.

This effective impulse is used in Eq. (3) to calculate the contribution of the time history response of each vibration mode in the total response. This response corresponds to one footfall strike.

$$v_n(t) = u_i u_j \frac{I_{eff}}{M_n} e^{-\zeta_n \omega_n t} \sin(\omega_{nd} t), \tag{3}$$

Here, $v_n(t)$ (m/s) is the contribution to the velocity response from mode n at each time step t, u_i and u_j are the mode shape amplitude at the node of application of the force and the node of interest, respectively, M_n (kg) is the modal mass of the mode n, ζ_n is the modal damping ratio, ω_n and ω_{nd} (rad/s) are the angular frequency and damped angular frequency of mode n, respectively.

The contribution of each mode in the total response, calculated using Eq. (3), should be determined individually for N vibration modes with a natural frequency up to twice the fundamental frequency. The total velocity response $v_t(t)$ is calculated using Eq. (4) based on the assumption that the structure remains linear during vibration, and therefore, the principle of superposition applies.

$$v_t(t) = \sum_{n=1}^{N} v_n(t), \tag{4}$$

The criterion of the vibration serviceability assessment for high-frequency floors is based on the maximum 1-s RMS of the total response calculated using Eq. (1).

3.2. Improved modelling procedure

Based on the analysis presented in Section 2, the key differences between the steps followed to derive Arup's model and its advanced version explained in the following sections are:

- The range of natural frequencies of the SDOF oscillators used to derive the present model is 14–40 Hz with an increment of 0.1 Hz, compared with 10–40 Hz used to derive Arup's model. This is to account for the proposed cut-off frequency of 14 Hz (Section 2.3).
- In the new model, SDOF simulations, which utilised continuously measured treadmill forces [15,16], were carried out to extract the peak velocities corresponding to 50 successive footfalls. These peak velocities are treated as the effective impulse (I_{eff}) explained in Eq. (3) but they belong to the improved model presented in this paper.
- Contrary to Arup's model, the damping effect is considered in the new model. This is to take into account the slight amplification of

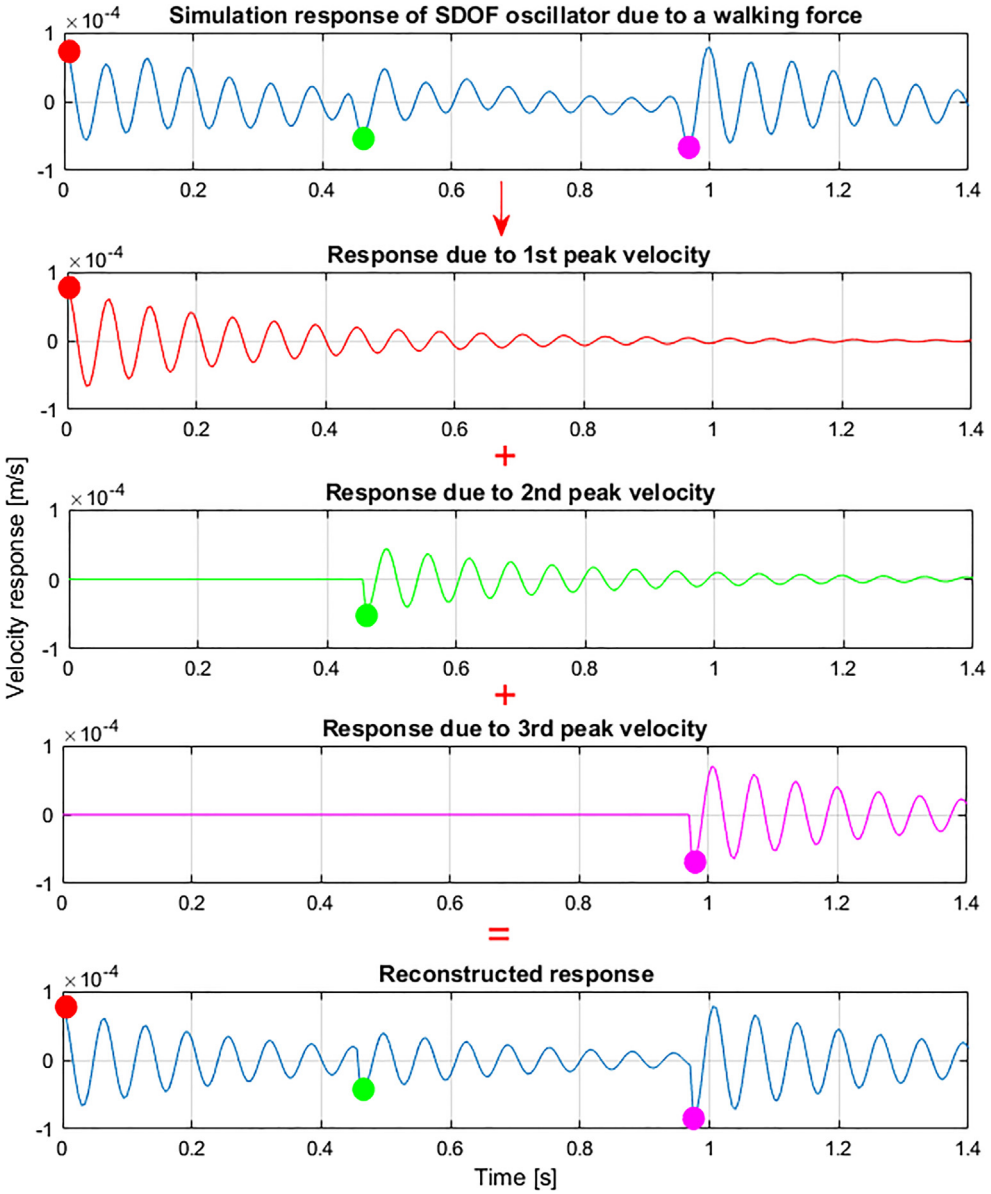

Fig. 5. Typical reconstructed vibration response from simulation of a walking force with pacing rate (f_p) of 2.0 Hz applied on SDOF oscillator with a natural frequency (f_n) of 16 Hz. Red, green and pink dots refer to the 1st, 2nd and 3rd peak velocities, respectively.

the vibration response of high-frequency floors induced by the near-resonance effects corresponding to the higher harmonics of walking loading, as explained in Section 2.

Apart from the above mentioned differences, the new model was derived using the same procedure as that used for Arup's model. The damping ratio was assumed 3% in the SDOF simulations, while the effect of other damping ratios is elaborated in Section 3.3.3. A time step of 0.005 s was used in the analysis. The total number of the peak velocities (effective impulses) obtained from the analysis is more than 900,000, i.e. 715 continuously measured walking forces [15,16], each comprising 50 footfalls, applied to 261 SDOF oscillators with natural frequencies in the range14–40 Hz and 0.1 Hz increments.

3.3. Formulation of the effective impulse

The peak velocities corresponding to a single footfall and multiple SDOF oscillators can be presented as a spectrum. Fig. 10 shows an example of this spectrum corresponding to one footfall within a continuous walking force, with a pacing rate of 2.25 Hz. For example, for this pacing rate there are 28 continuously measured walking force time histories in the database [15,16], each having 50 footfalls. This means there are 1400 spectra created and analysed for this pacing rate. The differences between these spectra can be explained by the inter- and intra-subject variabilities of human walking forces (Section 2.1). Hence, a statistical approach is utilised here to model the spectra as a function of SDOF natural frequency, pacing rate and damping ratio.

In Fig. 10 peaks can be noticed around integer multiples of the pacing rate due to resonance or near-resonance effects. This can be explained by the effect of harmonics of the walking excitation at integer multiples of pacing rates as explained in Section 2.2.

To simplify the modelling of the spectrum shown in Fig. 10, it was split into two components: a 'base curve' and an 'amplification factor' (grey curve and black dots, respectively, in Fig. 10). The base curve was assumed continuous across all SDOF frequencies, while the amplification factor was assumed to be present at locations of each integer multiple of the pacing rate (black dots in Fig. 10). The grey dots represent the locations where the amplification factor has no effect and its

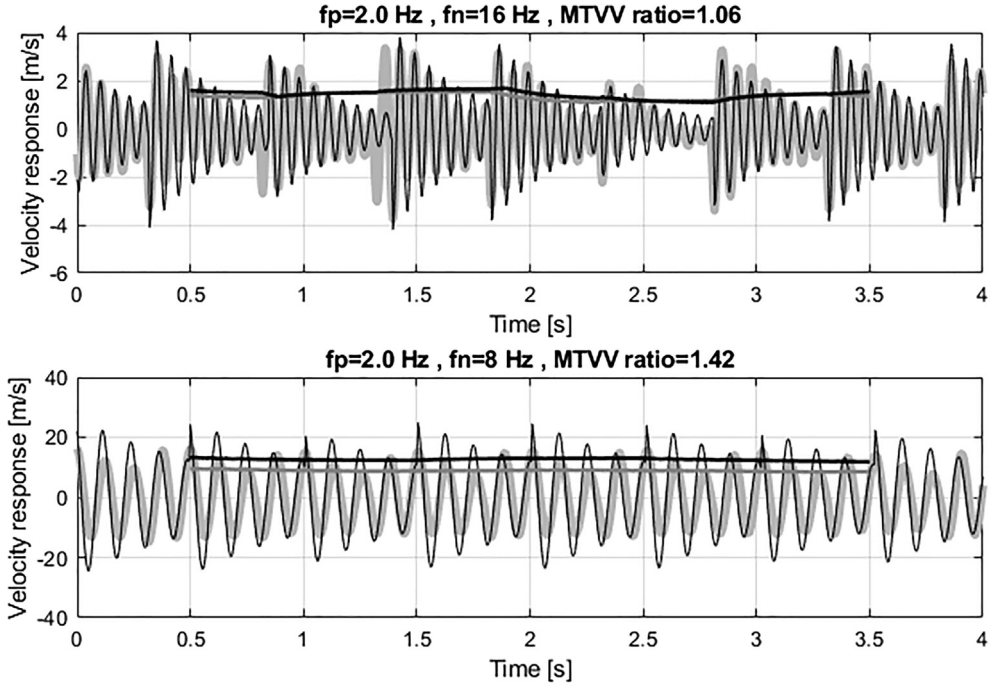

Fig. 6. Comparison between simulated (grey) and reconstructed (black) vibration responses with their corresponding 1-s running RMS for natural frequency (f_n) of 16 Hz (top) and 8 Hz (bottom).

location is assumed to be in the middle of each two successive integer multiples of pacing rate (subsequent pairs of the black dots). Between black and grey dots, the amplification factor can be assumed to change linearly and its value can be interpolated between them.

Hence, the peak velocity at each integer multiple of the walking frequency is theoretically equal to the base curve value at that natural frequency multiplied by the corresponding contribution of the amplification factor at the same natural frequency, as shown in Fig. 10.

A Matlab script was written to extract the amplification factor around each integer multiple of the pacing rate, while the base curve was constructed by connecting the grey dots linearly (Fig. 10). The base curve values $B(f_n,f_p)$ (m/s) and amplification factor $A_f(f_n,f_p)$ (dimensionless parameter) were assumed as functions of both the natural (f_n) and pacing (f_p) frequencies. Hence, the effective impulse can be mathematically described in Eq. (5).

$$I_{eff} = B(f_n,f_p)A_f(f_n,f_p)P_\zeta(f_p,f_n,\zeta), \tag{5}$$

where, $P_\zeta(f_p,f_n,\zeta)$is the damping factor (dimensionless parameter), which is described in Section 3.3.3.

In the remaining part of this section, the probability distributions used to fit $B(f_n,f_p)$ and $A_f(f_n,f_p)$ were chosen based on the Bayesian Information Criterion [28] and the parameter fitting is based on the Nonlinear Least Squares method [29].

3.3.1. Base curve

Fig. 11 shows that $B(f_n,f_p)$ values fit well a gamma distribution defined as [30]:

$$f(B(f_n,f_p)) = \frac{B(f_n,f_p)^{k-1}e^{-\frac{B(f_n,f_p)}{\theta}}}{\theta^k(k)}, \tag{6}$$

where $f(B(f_n,f_p))$ is the probability density function, k and θ are the shape and scale parameters and $\Gamma(k)$ is the gamma function evaluated at k.

The fitting process is repeated for 35,750 spectra (i.e. 715 walking force time histories, each comprising 50 footfalls). Values of the extracted parameters k and θ (dimensionless parameters) were then surface fitted as functions of f_n and f_p (measured in Hz) using polynomial and exponential forms, due to the shape of the data to be fitted. The fitting is shown in Fig. 12 and described by Eqs. (7) and (8).

$$k = 4.5-0.12f_n + 3f_p, \tag{7}$$

$$\theta = 0.08 + 2\frac{f_p^{3.3}}{f_n^{1.58}}, \tag{8}$$

3.3.2. Amplification factor

Values of amplification factors $A_f(f_n,f_p)$ follow the generalised extreme value distribution (Fig. 13), which probability density function $f(A_f(f_n,f_p))$is characterised by location μ, scale σ and shape τ parameters as described in Eq. (9) [31].

$$f(A_f(f_n,f_p)) = \frac{1}{\sigma}\tau\left[1+\tau\left(\frac{A_f(f_n,f_p)-\mu}{\sigma}\right)\right]^{-1-1/\tau} e^{\left\{-\left[1+\tau\left(\frac{A_f(f_n,f_p)-\mu}{\sigma}\right)\right]^{-1/\tau}\right\}} \tag{9}$$

The extreme probability distribution is fitted to all 35,750 spectra. The extracted values of μ, σ and τ (dimensionless parameters) are further fitted to surfaces as functions of f_n and f_p (measured in Hz). The results are illustrated in Fig. 14 and the mathematical formulation is described by Eqs. (10)–(12). Note that due to the shape of the fitting data, the exponential form best fitted μ and σ surfaces, while the polynomial function best fitted τ values.

$$\mu = 0.98 + 7.6\frac{f_p^{2.5}}{f_n^{1.82}}, \tag{10}$$

$$\sigma = -0.03 + 0.85\frac{f_p^{1.3}}{f_n}, \tag{11}$$

$$\tau = 0.18-0.00013f_n^2-0.015f_nf_p + 0.0004f_pf_n^2, \tag{12}$$

Interpolation of $A_f(f_n,f_p)$ should be considered if the natural frequency is not an integer multiple of the pacing rate (Fig. 10). For instance, if the natural frequency lies exactly in the middle of two successive integer multiples of the pacing rate, the amplification factor will

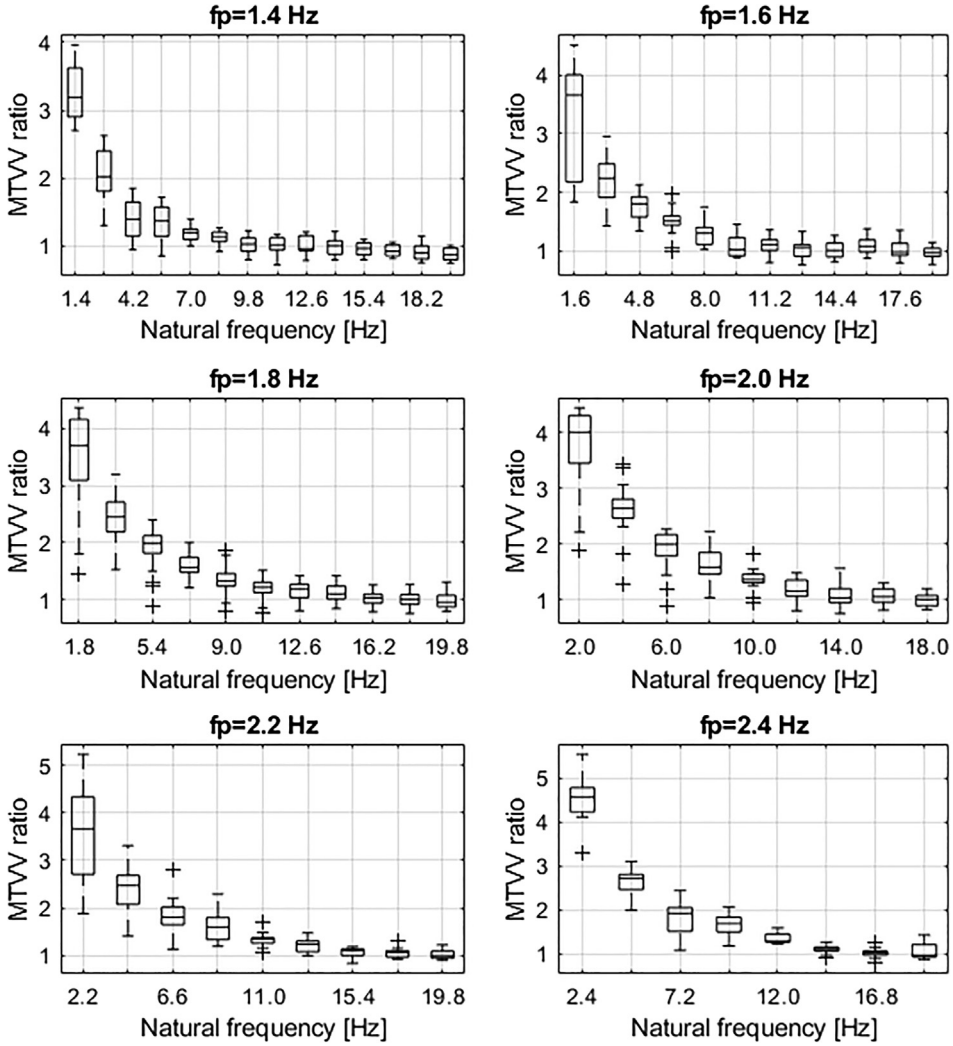

Fig. 7. MTVV ratio between simulated and reconstructed vibration responses at different pacing rates (f_p).

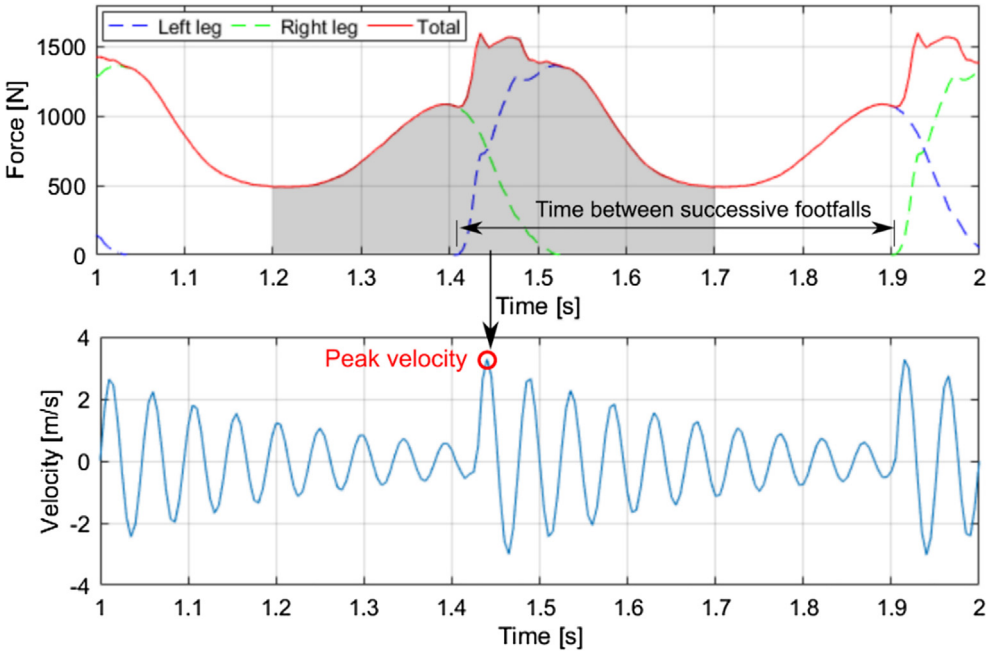

Fig. 8. Arup's approximation of the typical walking force (top) and its corresponding velocity vibration response (bottom).

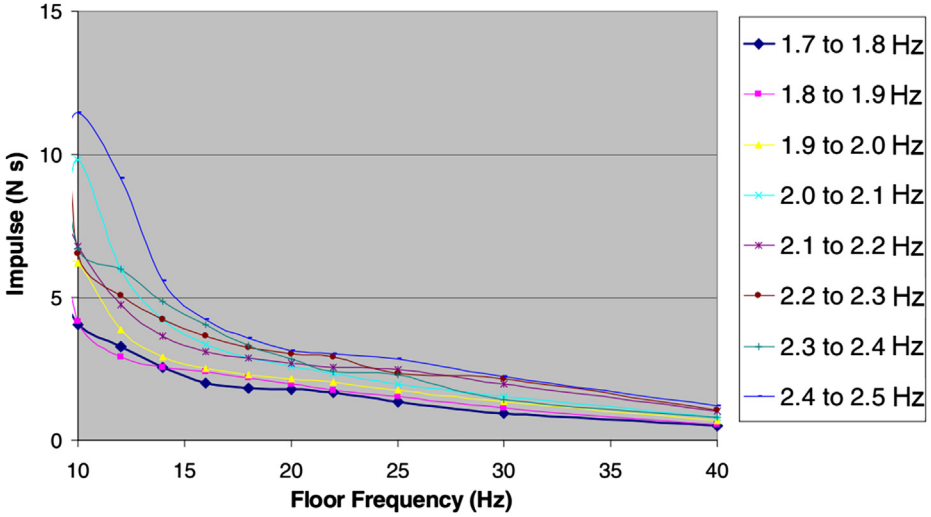

Fig. 9. Effective impulse derived from Kerr [25] footfall traces (after Willford et al. [35]).

have no effect on the response (i.e. $A_f(f_n,f_p) = 1.0$). This takes into account that the amplification factor has a reduced effect between the integer multiples of the pacing rate, as shown in Fig. 10.

3.3.3. Damping effect

A damping factor is developed in this section to scale amplification factor $A_f(f_n,f_p)$ to account for the effect of a floor near-resonance with the harmonics of walking excitation above 14 Hz and to account for damping ratios ζ of the SDOFs different from 3%. Hence, the numerical simulations presented in the previous section are repeated here to derive amplification factors $A_f'(f_n,f_p,\zeta)$ for damping ratios in the range 0.5%-6%, with an increment of 0.1%. The damping factor $P_\zeta(f_p,f_n,\zeta)$ can be expressed as:

$$P_\zeta(f_p,f_n,\zeta) = \frac{A_f(f_n,f_p)}{A_f'(f_n,f_p,\zeta)}, \tag{13}$$

The plane defined by Eq. (14) is fitted to $P_\zeta(f_p,f_n,\zeta)$ for different damping ratios:

$$P_\zeta(f_p,f_n,\zeta) = a + bf_p + cf_n, \tag{14}$$

where, a, b and c are the parameters of the equation (dimensionless parameters). Fig. 15 shows the fitted plane corresponding to a damping ratio of 5%.

Finally, values of the parameters a, b and c are curve fitted as functions of the damping ratio. The resulting curve fits are illustrated in Fig. 16 and described by Eqs. (15)–(17). The shapes of these equations are decided based on the trends observed in the data (Fig. 16).

$$a = 2.82 - 2.58\zeta^{0.1} \tag{15}$$

$$b = -0.0174 + \frac{0.38}{e^{100\zeta}} \tag{16}$$

$$c = 0.0028 - \frac{0.0138}{e^{50\zeta}} \tag{17}$$

According to Eq. (14), the range of $P_\zeta(f_p,f_n,\zeta)$ is 0.86–1.72. The lower and upper limits correspond to $f_p = 2.5$ Hz, $f_n = 14$ Hz and $\zeta = 6\%$ and $\zeta = 0.5\%$, respectively. It is assumed that the damping factor $P_\zeta(f_p,f_n,\zeta)$ has the highest effect when f_n is an integer multiple of f_p due to the near-resonant effect with the higher harmonics of walking, as was the case with $A_f(f_n,f_p)$ in the previous section. Hence, if the natural frequency is not an integer multiple of the pacing rate, $P_\zeta(f_p,f_n,\zeta)$ need to be interpolated in the same way as $A_f(f_n,f_p)$.

3.4. Implementation of the new model

Vibration serviceability assessment of a high-frequency floor using the new model takes the following steps:

- The modal properties are derived from either modal testing or a finite element model (FEM) of the floor.
- The walking path, pacing rate and its corresponding walking speed or step length can be utilised to calculate the time that a walking

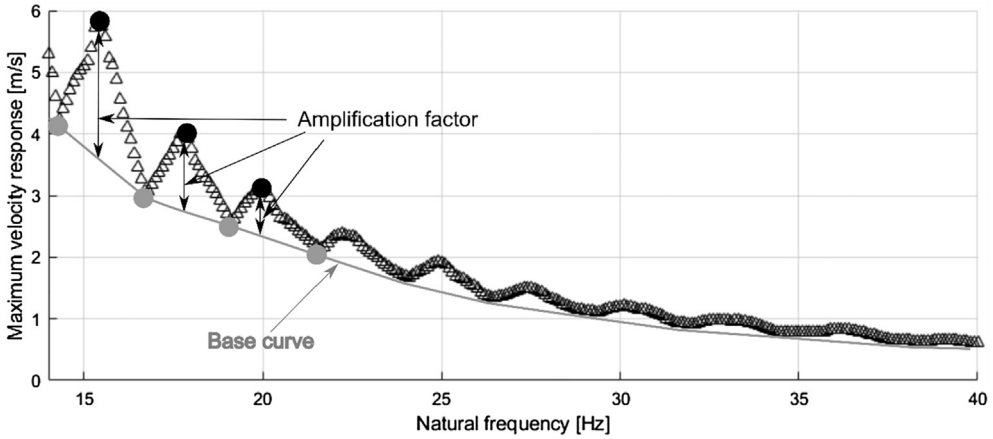

Fig. 10. Spectrum (black triangles) of peak velocity response corresponding to one footfall within a continuous walking force with a pacing rate of 2.25 Hz.

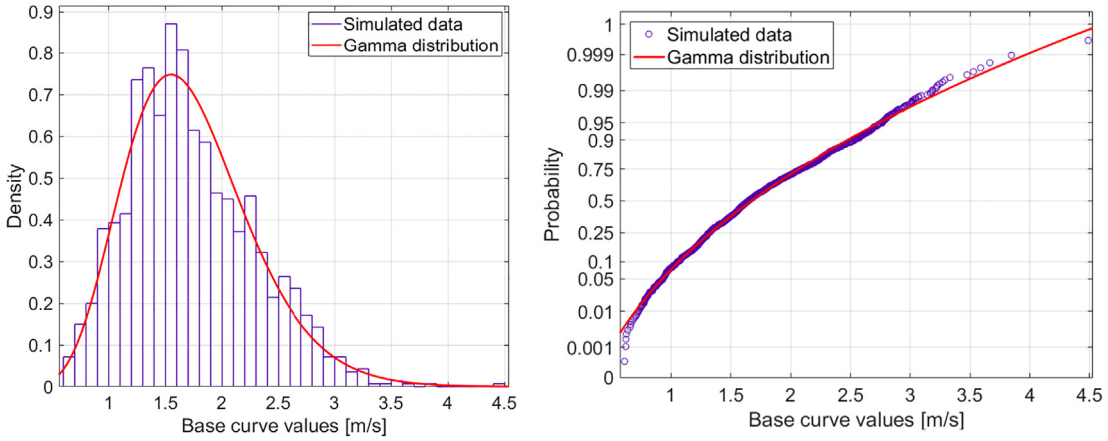

Fig. 11. Probability density function (left) and cumulative probability density function (right) derived using best fit of gamma distribution for a sample of base curve values corresponding to a pacing rate 2.25 Hz and SDOF natural frequency 24.8 Hz.

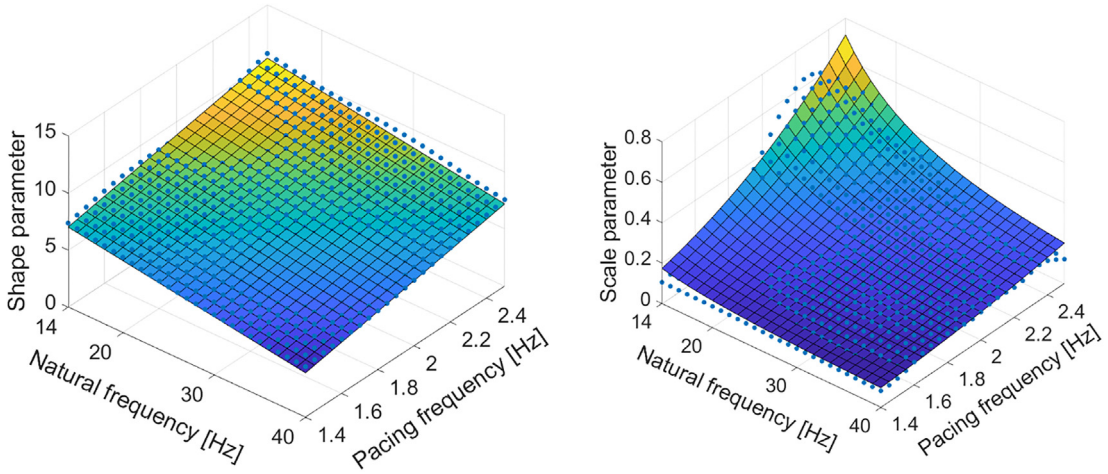

Fig. 12. Best fits of the shape (left) and scale (right) parameters for the gamma distribution.

person spends while walking on the floor. This is necessary to determine the number of footfalls and the duration of the vibration response. Further discussion about deciding an appropriate pacing rate and walking path is beyond the scope of this paper. However, a reader is advised to generate value of the pacing rate based on probability density functions available in the literature [32].

- For each vibration mode, Eqs. (7), (8), (10)–(12) are used to calculate the distribution parameters related to the gamma and the generalised extreme value distributions. Random values of these distributions are generated based on Eqs. (6) and (9) corresponding to $A_f(f_n f_p)$ and $B(f_n f_p)$, respectively. The number of the generated values is the same as the number of footfalls calculated above. The effect of damping is considered by calculating $P_\zeta(f_p f_n, \zeta)$using Eq. (14), which parameters can be calculated using Eqs. (15)–(17). The

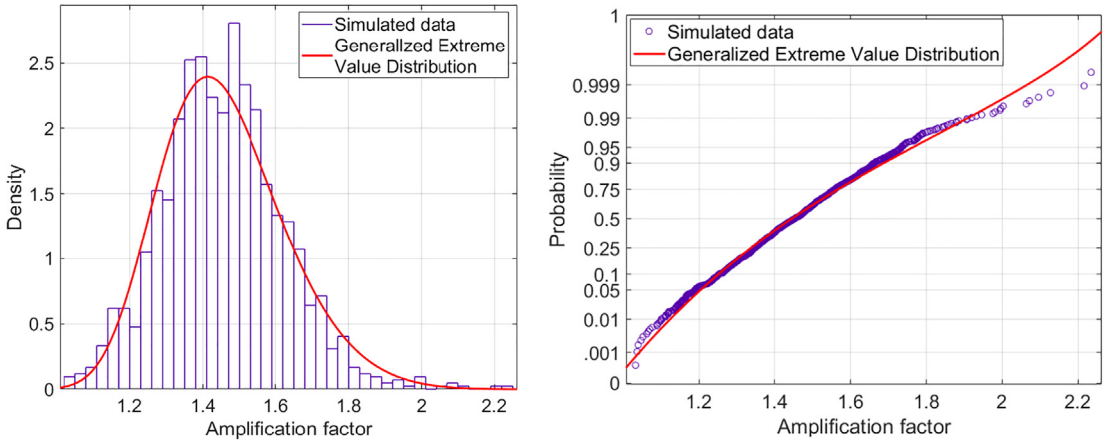

Fig. 13. Probability density (left) and cumulative probability density (right) functions using best fit of generalised extreme value distribution for a sample of amplification factor values corresponding to a pacing rate of 2.25 Hz and natural frequency of 24.8 Hz.

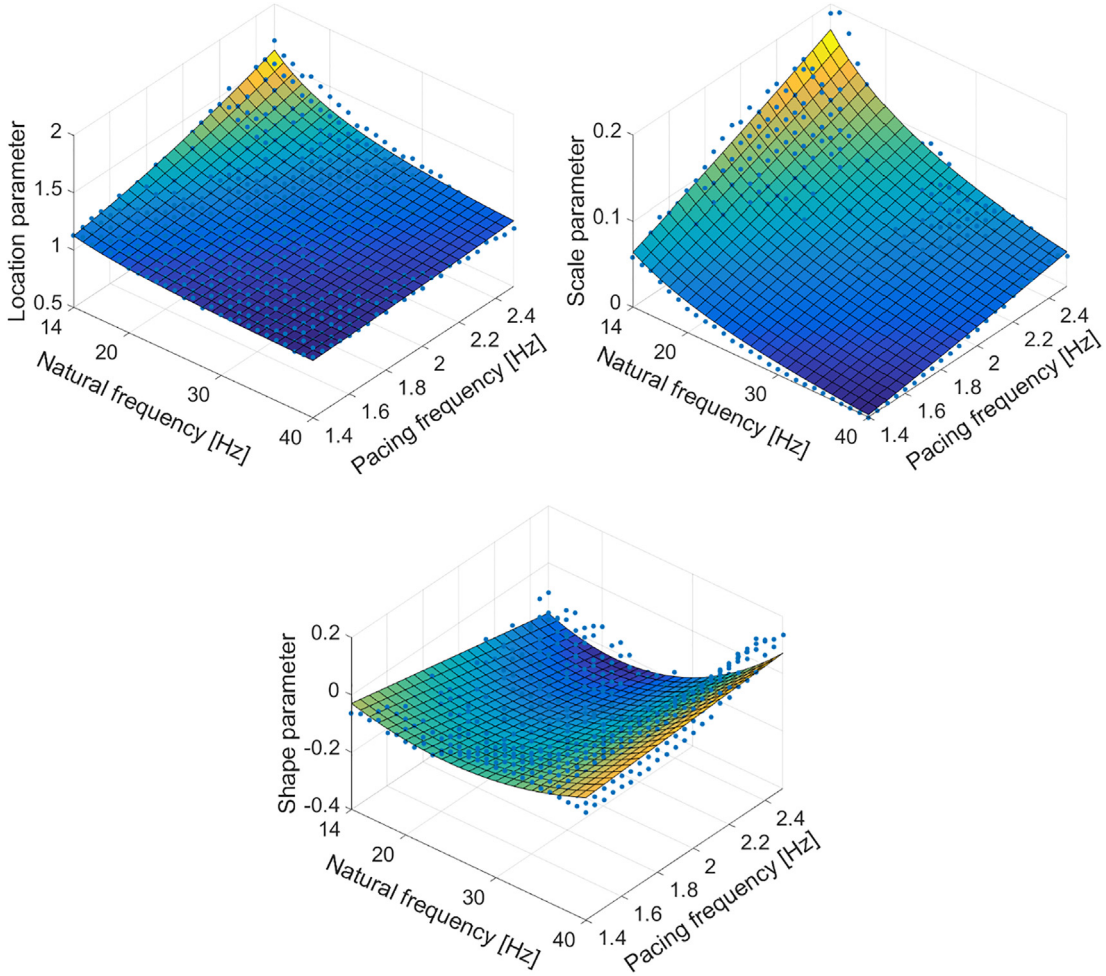

Fig. 14. Best fits of the location (top left), scale (top right) and shape (bottom) parameters for the generalised extreme value distribution.

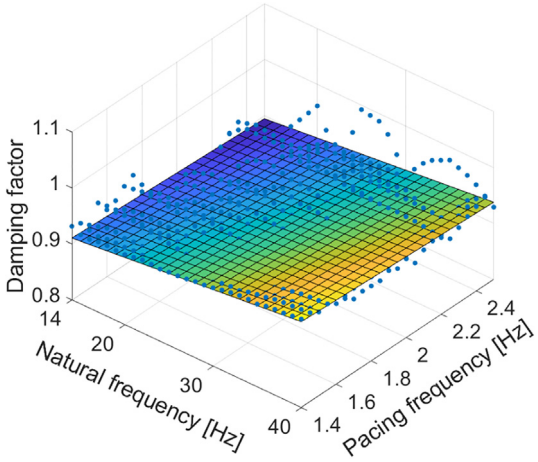

Fig. 15. Best fit of the damping factors corresponding to a damping ratio of 5%.

generated values of $A_f(f_n,f_p)$ and $P_\zeta(f_p,f_n,\zeta)$ need to be scaled depending on the natural frequency of the considered vibration mode and the pacing rate, as explained in Section 3.3.2 and Fig. 10.

- The effective impulse I_{eff} corresponding to each footfall can be determined using Eq. (5). The time history of decaying vibration response due to each effective impulse is calculated utilising Eq. (3) and the modal properties of each mode under consideration. The total time history response due to each mode can be obtained when the decaying responses are sequenced one after another to form a continuous response time history for the duration of walking. The time between each two successive footfalls needs to be consistent with the pacing rate. The residual of each decaying response at the beginning of the next footfall is assumed to be zero.
- The total response corresponding to the contribution from all vibration modes having frequencies up to twice the fundamental frequency is calculated using Eq. (4). This number of vibration modes is adopted from the Arup's model.

By following the above mentioned procedure, a single response time history can be obtained. To consider the statistical nature of $A_f(f_n,f_p)$ and $B(f_n,f_p)$, a sufficient number of responses needs to be generated as explained below. This number of samples n is defined by Eq. (18) [33].

$$n = \left(\frac{s}{SE_{\bar{x}}}\right)^2, \tag{18}$$

where, s is the standard deviation of the population and $SE_{\bar{x}}$is the standard error of their mean.

In this study, the samples are a set of MTVV velocity calculated following the above mentioned procedure, while the population refers to all possible MTVV velocities. As the standard deviation of the population s is unknown, it is estimated to be the standard deviation of the samples. Assuming the samples are independent and identically distributed, there is a 95% chance that their mean is within the population mean ∓ a tolerance of $1.96SE_{\bar{x}}$ [33]. This tolerance should be specified based on the required accuracy [33]. The authors suggest using a tolerance value of 1% of the mean of the samples.

Hence, the sufficient number of responses can be found in an

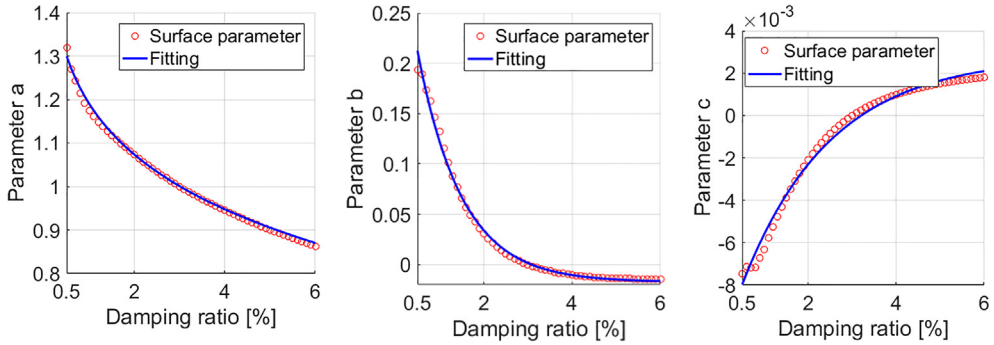

Fig. 16. Fitting parameters a (left), b (middle) and c (right).

iterative approach. After generating each sample (MTVV velocity), the sufficient number of samples n can be calculated using Eq. (18) and compared with the actual number of generated samples. When Eq. (18) is fulfilled (i.e. the number of generated samples is equal or higher than the sufficient number of samples n) the simulations can be stopped.

Finally, the cumulative distribution function (CDF) of the MTVV velocity, corresponding to the generated responses, can be obtained and the vibration serviceability assessment can be carried out based on the desired probability. The whole process explained in this section is summarised in Fig. 17.

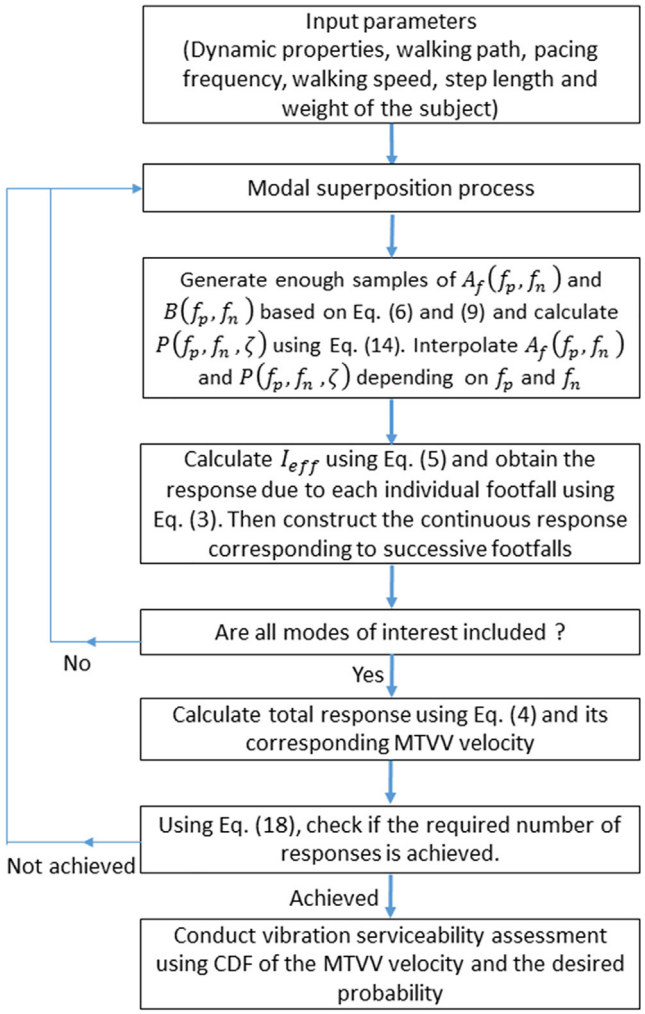

Fig. 17. Implementation procedure of the new model.

4. Verification

The performance of the model elaborated in the previous section is verified here against numerical simulations (Section 4.3) of the vibration response calculated using the measured treadmill forces (Section 2.1) and an FEM of a high-frequency floor (Section 4.1). Simulations are also carried out using the original Arup model (Section 4.3) for comparison (Section 4.4).

4.1. Finite element model

The FEM utilised in this section is developed using ANSYS FE software [34] and is updated to match the experimentally measured modal properties of the corresponding real floor (Fig. 18). The floor is a 58 m × 14 m composite slab supported by steel beams and columns. The slab has a concrete deck with thickness 130 mm and it was modelled using a shell element (SHELL181 in ANSYS) assuming isotropic behaviour with a mesh size of 0.5 m. BEAM188 element was used to model the supporting steel beams and columns. The elastic modulus used to model the concrete and steel materials are 38 GPa and 210 GPa, while their corresponding Poisson's ratios are 0.2 and 0.3, respectively. The structure has a maximum span of 7.0 × 6.0 m and similar (but not identical) structural configuration between its two wings (left and right). The columns were fixed at the far ends and the lateral movement of the floor was restrained at the perimeter of the floor.

Fig. 19 shows the first six vibration modes of the structure. While the first 18 vibration modes have contributions from either the left or the right wing of the structure, the other eight vibration modes have contributions from both wings. The dynamic properties of all vibration modes with a natural frequency up to twice the fundamental frequency (26 vibration modes) were extracted from the FEM and used in the analysis presented in the next section.

4.2. Simulations based on measured walking forces and FEM

The simulations are carried out using 60 measured forces (Section 2.1) due to people walking at six walking frequencies (i.e. ten walking forces for each pacing rate 1.4, 1.6, 1.8, 2.0, 2.2 and 2.4 Hz) representing slow to fast walking scenarios.

A walking path expected to produce the maximum response is specified before performing the simulations (Fig. 19). A constant value of 0.75 m was used for the step length. Unity-scaled (normalised to a maximum value of 1.0) mode shapes $\{\phi_r\}$ were used to calculate the modal force time histories $P_r(t)$ for each mode r for the walking force moving along the walking path, as described in Eq. (19):

$$P_r(t) = f(t)\phi_r(v.\,t), \tag{19}$$

where, $f(t)$ is the physical walking force, t is time, v is the constant walking speed, $r = 1,2,...$ refers to different modes of vibration and $\phi_r(v.\,t)$ is amplitude of the mode shape r at the location of the pedestrian at time t. Essentially Eq. (19) describes scaling of walking force

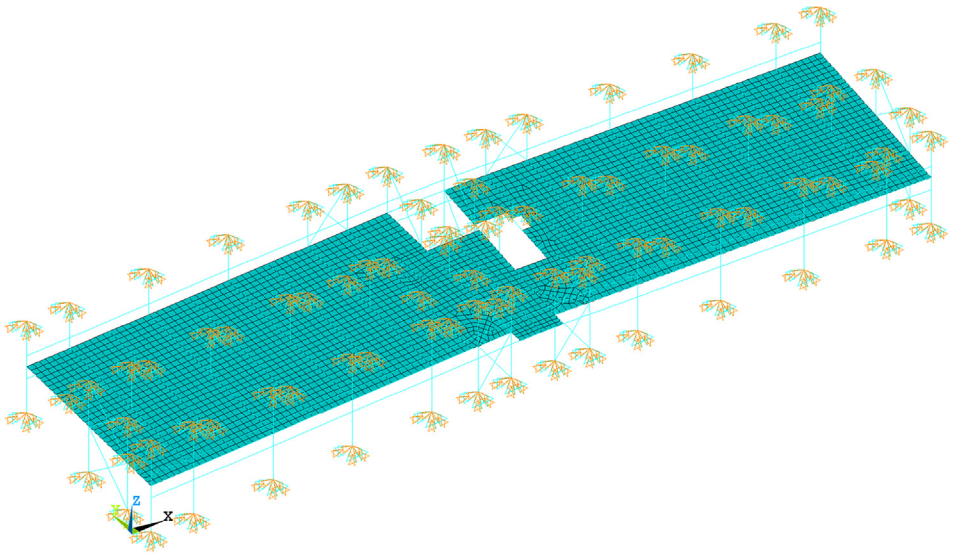

Fig. 18. FEM of the floor structure.

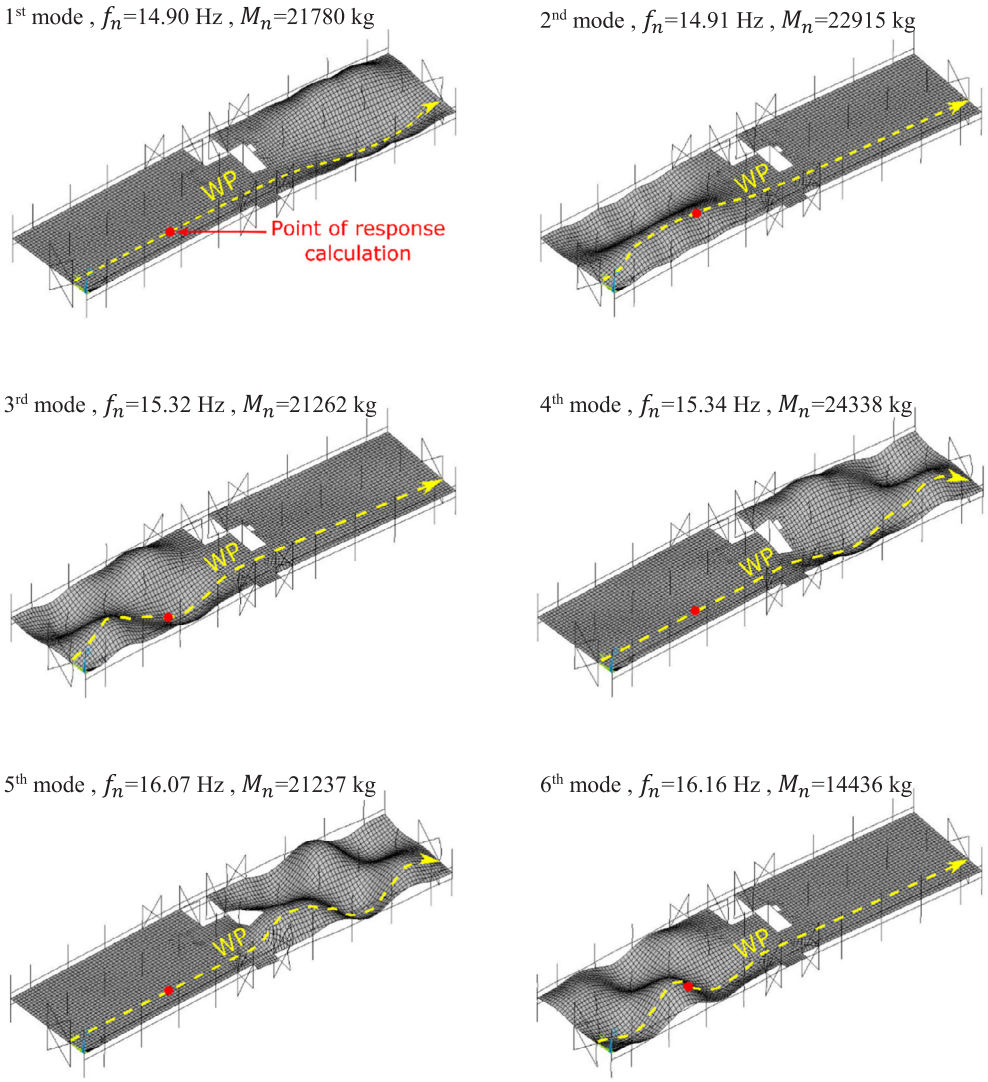

Fig. 19. Mode shapes, natural frequencies (f_n) and modal masses (M_n) of the first six modes showing the walking path (WP) (dashed yellow line) and the point of the response calculations (red dot).

$f(t)$ by mode shape amplitudes $\phi_r(v.\ t)$ along the walking path. Due to the discrete locations of the nodes, the amplitudes of the unity-scaled mode shapes corresponding to the location of the pedestrian at each time step were obtained by interpolation.

The contribution of each mode in the total response was obtained by applying the modal force time history to a SDOF oscillator having the same modal properties as that extracted from the FEM. The Newmark integration method was used to solve the corresponding equation of motion with a time step of 0.005 s. The modal damping ratio was assumed 3% in all simulations. The vibration responses were calculated at a node which has contributions from as many vibration modes as possible (red dot in Fig. 19). Hence, the contribution of each mode in the total response was multiplied by its corresponding mode shape value at that node (u_j). The total responses were determined based on the superposition principle, i.e. by adding responses from all vibration modes having a natural frequency up to twice the fundamental frequency.

This procedure was repeated to simulate the vibration response due to each measured walking force. Therefore, there are 60 vibration response time histories, here called “oscillator based responses”, used in the next section for comparison with the vibration responses calculated using both the new model and Arup’s model.

4.3. Calculated responses using the new model and Arup’s model

The same walking path, pacing rates, step length and modal properties from the previous section were used here to calculate the responses, using both the newly proposed model and Arup’s model.

For the new model, the procedure described in Section 3.4 was followed to estimate the vibration response time histories and their corresponding MTVV velocity. After generating each response, an estimation of the required number of generated responses, according to Eq. (18), is obtained and compared with the actual number of generated responses, as shown in Fig. 20.

The vibration response using Arup’s model was estimated in a similar procedure. The main difference is that the effective impulse is calculated based on Eq. (2) instead of Eq. (5).

4.4. Results and comparison

Examples of velocity time history responses calculated using the oscillator based simulations and the new model are presented in Fig. 21. Based on the visual inspection, the responses are apparently very similar.

A numerical comparison between the vibration responses can be made using their cumulative probability distribution. Fig. 22 shows the overlaid plot of the cumulative probability distribution corresponding to each vibration response time history obtained using the oscillator based simulations, the new model and Arup’s model.

This figure shows that the vibration response levels calculated using the new model (light grey curves in Fig. 22) are relatively close to that obtained from the oscillator based simulations (dark grey curves in Fig. 22). The vibration responses calculated using Arup’s model slightly overestimate the responses corresponding to the pacing rates of 1.4 Hz and 1.6 Hz, while less conservative results were obtained for vibration responses corresponding to other pacing rates (Fig. 22).

A more obvious and appropriate comparison between the considered vibration responses can be carried out using the MTVV of the velocity responses. Fig. 23 presents the cumulative probability distribution of the MTVV velocity corresponding to the generated responses using the new model. This represents the MTVV velocity prediction range of the proposed model. For comparison purposes, the projections of the MTVV velocity, corresponding to the responses obtained using the oscillator based simulations and Arup’s model, on the cumulative probability distribution in Fig. 23 were illustrated in the same figure.

Most of the MTVV velocity corresponding to the oscillator based simulations are within the predicted range of the vibration responses obtained using the new model (Fig. 23). Only four vibration responses (out of 60) obtained from the oscillator based simulations are outside but relatively close to the predicted range of the vibration levels calculated using the new model. Ideally, the MTVV velocity of the oscillator based simulations should be clustered around vibration levels corresponding to a cumulative probability distribution value of 0.5 (Fig. 23). This is broadly achieved by most of the simulated MTVV velocity values (dashed grey lines in Fig. 23).

Arup’s methodology for vibration prediction has an implicit 75% chance of non-exceedance probability for a certain vibration level as explained in Section 3.1. This implies that the MTVV velocity corresponding to the responses obtained using Arup’s model should be higher than that corresponding to seven responses (out of 10) obtained

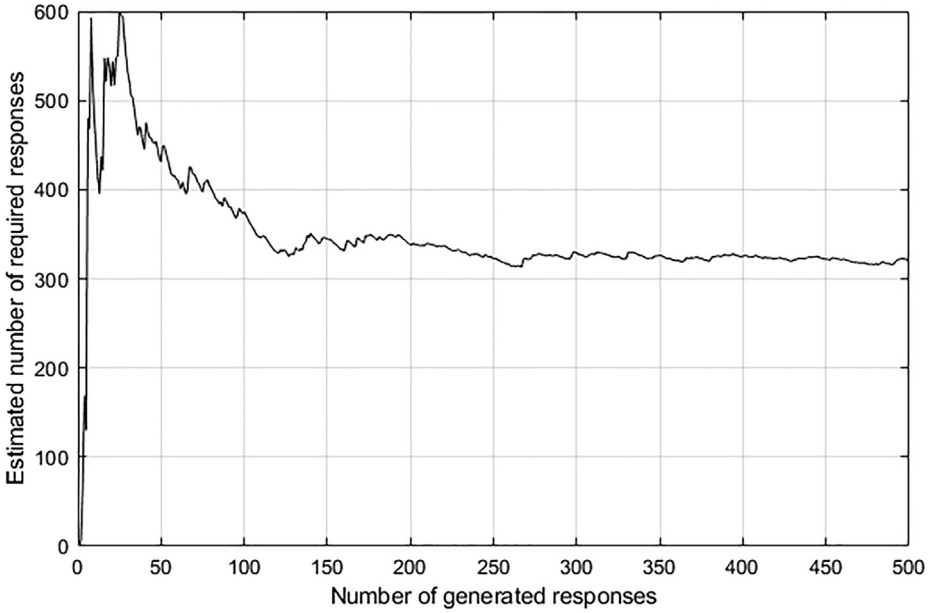

Fig. 20. Stability of the estimated number of the required simulations related to the response calculation at pacing rate of 1.4 Hz. The required number of generated responses was achieved after 326 iterations.

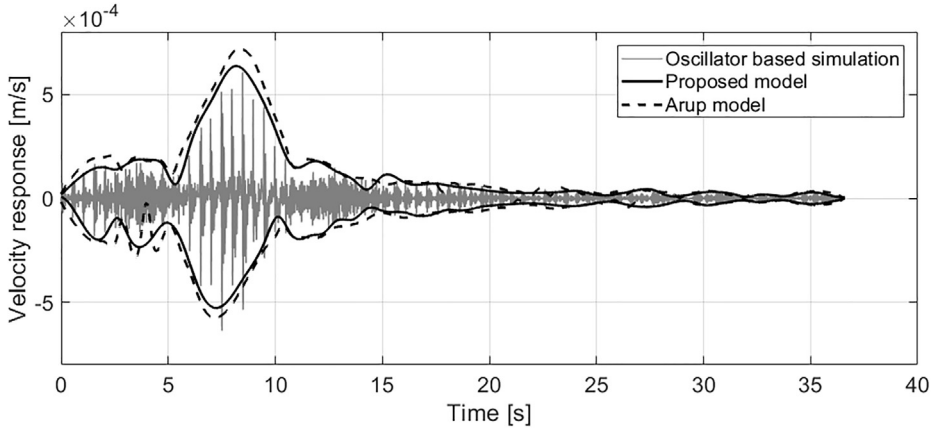

Fig. 21. Time-history response samples from the oscillator based simulations, the new model and Arup's model corresponding to a pacing rate of 2.0 Hz. For the responses calculated using the new model and Arup's model, only their envelopes are shown in this figure for comparison purposes.

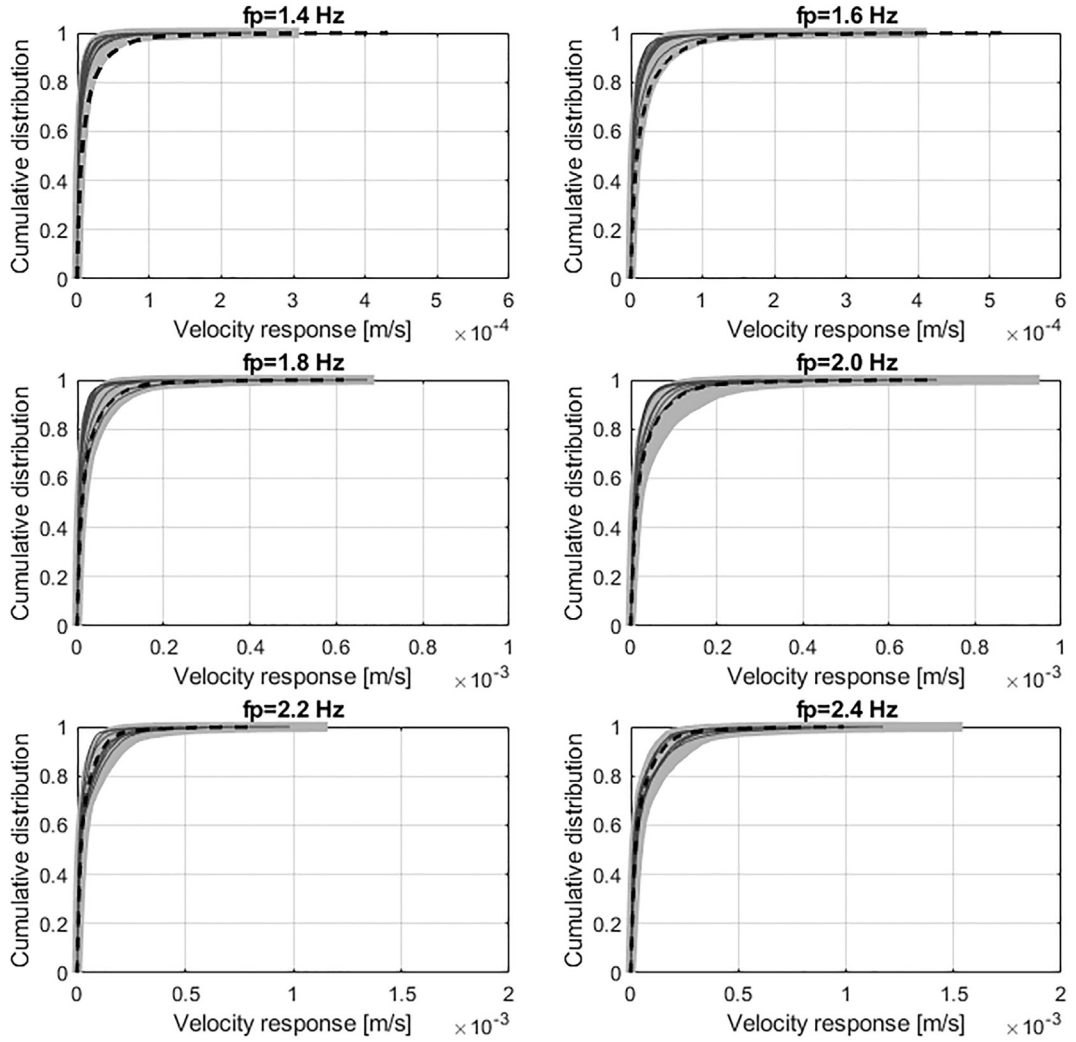

Fig. 22. Cumulative probability distribution function of the time history responses obtained from the new model (light grey curves), oscillator based simulations (dark grey curves) and Arup's model (dashed black curves).

from the oscillator based simulations related to each pacing rate. By comparing these MTVV velocity values, it is obvious that the vibration levels calculated using Arup's model are significantly overestimated for low pacing rates (1.4 Hz and 1.6 Hz) and slightly underestimated for a high pacing rate (2.4 Hz). Closer vibration levels were obtained for responses corresponding to pacing rates 1.8 Hz and 2.0 Hz (Fig. 23). The same trend can be observed when they are compared with the MTVV velocity corresponding to the new model (Fig. 23).

5. Discussion and conclusions

This paper presents an improved version of Arup's approach for the

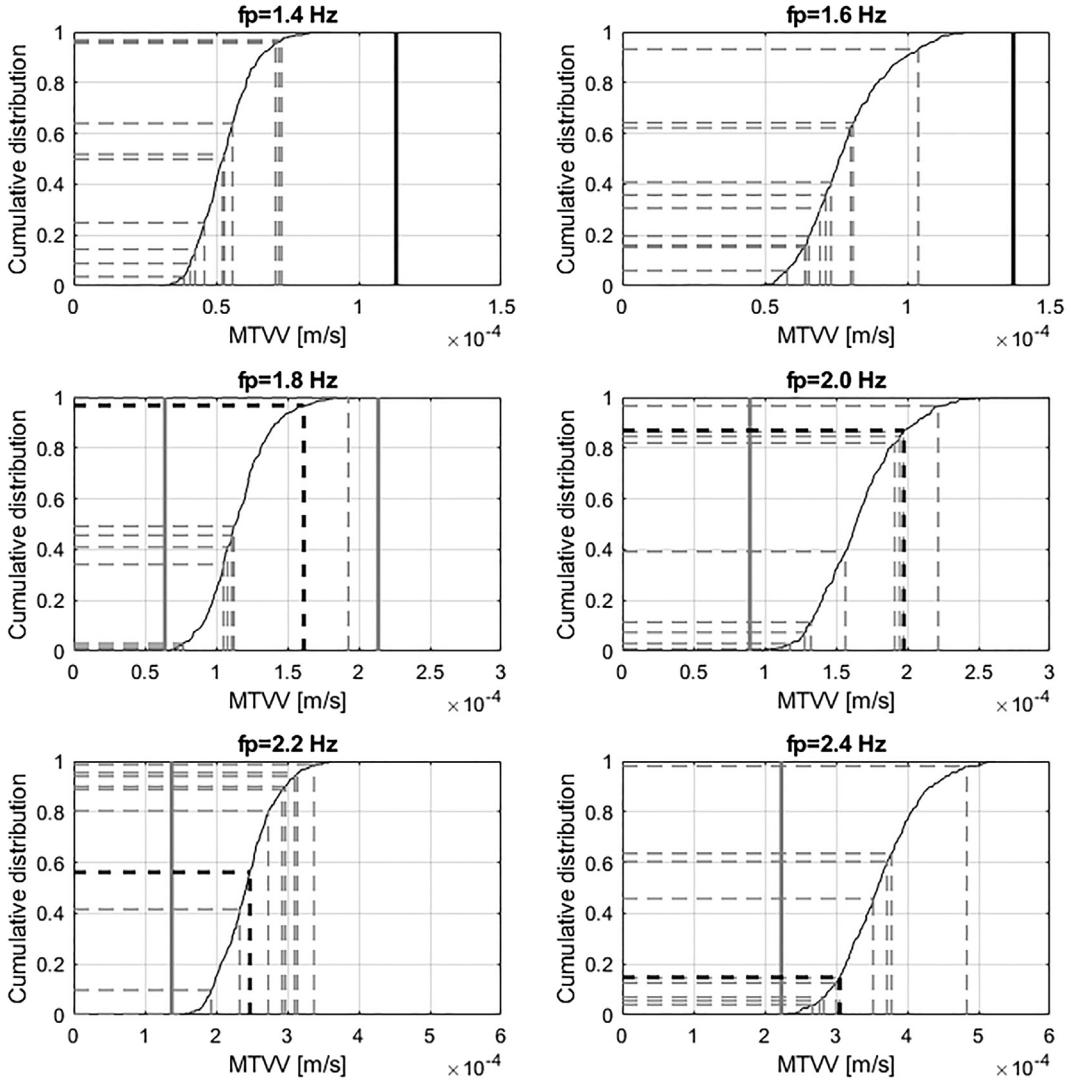

Fig. 23. MTVV velocity of the time history responses obtained from the new model (black thin curves), Arup's model (black thick lines) and the oscillator based simulations (grey lines). Solid vertical lines represent the values outside the ranges of the new model.

vibration serviceability assessment of high-frequency floors. The main advances are the new cut-off frequency of 14 Hz rather than 10 Hz between low- and high-frequency floors and the probabilistic rather than deterministic approach to modelling individual walking loading. Note that using cut-off frequency 14 Hz in the existing models for high-frequency floors (including Arup's model) may not be appropriate, as they were developed using simulations of different oscillators than in this study.

Another key advantage of the proposed force model is its capability to provide probability-based vibration serviceability assessment related to any given probability of exceedance of the floor vibration levels. This is far more flexible than Arup's original model providing vibration levels corresponding to 75% probability of non-exceedance. The probabilistic approach of the proposed individual walking loading and the related criterion for assessing vibration serviceability describes better the stochastic nature of human-induced vibrations than that of the existing model.

The simulation results showed that the new model can predict the vibration levels for more than 90% of cases. Those outside the range showed vibration levels mostly below (yet close to) their targets (Fig. 23). On the other hand, Arup's model tends to overestimate the response for low pacing rates, while a slight underestimation of the responses was noticed for high pacing rates. The best performance of Arup's model was observed for pacing rates corresponding to an average walking speed (i.e. 1.8 Hz and 2.0 Hz). This is in line with previous findings that Arup's model can underestimate the response for high-frequency floors with relatively low fundamental frequency and high pacing rate [14]. The reason for this could be related to using synthetic rather than continuously measured walking forces [15,16] and the range of the SDOF frequencies used to derive the model.

As the new model requires repetitive simulations, vibration serviceability assessment in design practice would benefit from a computer software where the results can be obtained within a few seconds on a standard PC configuration. In future this approach could also involve in the calculations statistical treatment of walking paths and other force parameters, such as pacing rate and body weight. Finally, the new model needs to be verified against vibration serviceability surveys of real high-frequency floors when occupied by walking people.

Acknowledgements

The authors would like to acknowledge the College of Engineering, Mathematics and Physical Sciences in the University of Exeter for the financial support provided for the PhD programme of the first author. The authors would also like to acknowledge the UK Engineering and Physical Sciences Research (EPSRC) for the following research grants:

- Platform Grant EP/G061130/2 (Dynamic performance of large civil engineering structures: an integrated approach to management, design and assessment) and.
- Standard Grant EP/I029567/1 (Synchronization in dynamic loading due to multiple pedestrians and occupants of vibration-sensitive structures).

References

[1] Racic V, Pavic A. Mathematical model to generate asymmetric pulses due to human jumping. ASCE J Eng Mech n.d. 135:1–6.
[2] Middleton CJ, Brownjohn JMW. Response of high frequency floors: A literature review. Eng Struct 2010;32:337–52.
[3] BSI. UK national annex to eurocode 1: actions on structures - Part 2: traffic loads on bridges. vol. NA to BS E. British Standards Institution; 2008.
[4] Ungar EE, White RW. Footfall-induced vibrations of floors supporting sensitive equipment. Sound Vibration 1979:10–3.
[5] Galbraith FW. Ground loading from footsteps. J Acoustical Soc Am 1970;48:1288. http://dx.doi.org/10.1121/1.1912271.
[6] Amick H, Hardash S, Gillett P, Reaveley RJ. Design of stiff, low-vibration floor structures. In: Proceedings of international society for optical engineering, vol. 1619. San Jose, San Jose, CA: SPIE; 1991. p. 180–91.
[7] Murray TM, Allen DE, Ungar EE. Floor vibrations due to human activity - AISC DG11. vol. DG-11. 1st ed. American Institute of Steel Construction; 1997.
[8] Fanella DA, Mota M. Design guide for vibrations of reinforced concrete floor systems. First edit. CRSI; 2014.
[9] Wyatt TA, Dier AF. Building in steel, the way ahead. In: International symposium: building in steel, the way ahead; 1989.
[10] Wyatt TA. Design guide on the vibration of floors SCI P076. London: The Steel Construction Institute, Construction Industry Research and Information Association; 1989.
[11] Hanagan LM, Murray TM. Active control approach for reducing floor vibrations. J Struct Eng 1997;123:1497–505. http://dx.doi.org/10.1061/(ASCE)0733-9445(1997) 123:11(1497).
[12] Liu D, Davis B. Walking vibration response of high-frequency floors supporting sensitive equipment. J Struct Eng 2014. http://dx.doi.org/10.1061/(ASCE)ST.1943-541X.0001175. 4014199-1–04014199-10.
[13] Ellis BR, Ji T, Littler JD. The response of grandstands to dynamic crowd loads. Proc ICE: Struct Build 2000;140:355–65.
[14] Brownjohn JMW, Middleton CJ. Procedures for vibration serviceability assessment of high-frequency floors. Eng Struct 2008;30:1548–59.
[15] Racic V, Brownjohn JMW. Mathematical modelling of random narrow band lateral excitation of footbridges due to pedestrians walking. Comput Struct 2012;90–91:116–30. http://dx.doi.org/10.1016/j.compstruc.2011.10.002.
[16] Racic V, Brownjohn JMW. Stochastic model of near-periodic vertical loads due to humans walking. Adv Eng Inf 2011;25:259–75. http://dx.doi.org/10.1016/j.aei.2010.07.004.
[17] Brownjohn JMW, Pavic A, Omenzetter P. A spectral density approach for modelling continuous vertical forces on pedestrian structures due to walking. Can J Civ Eng 2004;31:65–77. http://dx.doi.org/10.1139/l03-072.
[18] Živanovic S, Pavic A. Probabilistic modeling of walking excitation. J Constr Steel Res 2009;23:132–43.
[19] Brownjohn JMW, Racic V, Chen J. Universal response spectrum procedure for predicting walking-induced floor vibration. Mech Syst Sig Process 2015:1–15. http://dx.doi.org/10.1016/j.ymssp.2015.09.010.
[20] Willford MR, Young P. Improved methodologies for the prediction of footfall-induced vibration. In: Proceedings of the sixth European conference on structural dynamics EURODYN; 2005.
[21] Willford MR, Young P, Field C. Predicting footfall-induced vibration: Part 2. Struct Build 2007;160:73–9.
[22] Pavic A, Reynolds P, Prichard S, Lovell M. Evaluation of mathematical models for predicting walking-induced vibrations of high-frequency floors. Int J Struct Stab Dyn 2003;3:107–30. http://dx.doi.org/10.1142/S0219455403000756.
[23] Ohlsson S V. Floor vibrations and human discomfort. Chalmers University of Technology; 1982.
[24] Eriksson P-E. Vibration of low-frequency floors - dynamic forces and response prediction; 1994.
[25] Kerr SC. Human induced loading on staircases. PhD Thesis. University College London, Mechanical Engineering Department, London, UK; 1998.
[26] Murray TM, Allen DE, Ungar EE, Davis DB. Vibrations of Steel-Framed Structural Systems Due to Human Activity: AISC DG11 Second Edition; 2016.
[27] Pavic A, Willford MR. Vibration serviceability of post-tensioned concrete floors - CSTR43 App G. Appendix G in post-tensioned concrete floors design handbook - technical report 43 2005:99-107.
[28] Schwarz G. Estimating the dimension of a model. Ann Statistics 1978;6:461–4. http://dx.doi.org/10.1214/aos/1176344136.
[29] Teunissen PJG. Nonlinear least squares. Manuscripta Geodaetica 1990;15:137–50.
[30] Scheaffer R, McClave J, Franklin C. Probability and statistics for engineers. Fifth edit Boston, MA, USA: Cengage Learning; 2010.
[31] Kotz S, Nadarajah S. Extreme value distributions 2000. http://dx.doi.org/10.1007/978-3-642-04898-2.
[32] Racic V, Pavic A, Brownjohn JMW. Experimental identification and analytical modelling of human walking forces: Literature review. J Sound Vib 2009;326:1–49. http://dx.doi.org/10.1016/j.jsv.2009.04.020.
[33] Rothrock L, Narayanan S. Human-in-the-loop simulations, methods and practice. London: Springer; 2011. http://dx.doi.org/10.1007/978-0-85729-883-6.
[34] ANSYS Inc. ANSYS® Academic Research, Release 14.5 2015.
[35] Willford MR, Field C, Young P. Improved methodologies for the prediction of footfall-induced vibration. Architectural engineering conference, Omaha, Nebraska, United States; 2006. doi:http://dx.doi.org/10.1061/40798(190)17.
[36] Ohlsson S V. Ten years of floor vibration research - a review of aspects and some results. In: Proceedings of the symposium/workshop on serviceability of buildings (movements, deformations, vibrations), vol. 1, Ottawa, Canada; 1988. p. 419–34.
[37] Allen DE, Murray TM. Design criterion for vibrations due to walking. Eng J AISC 1993;30:117–29.
[38] Willford MR, Young P. A design guide for footfall induced vibration of structures - CCIP-016. Slough: The Concrete Centre; 2006.
[39] Smith AL, Hicks SJ, Devine PJ. Design of floors for vibration - A new approach SCI P354, Revised Ed. vol. SCI P354. The Steel Construction Institute; 2009.